

Deep Two-way Matrix Reordering for Relational Data Analysis

Chihiro Watanabe^{*1} and Taiji Suzuki^{†1,2}

¹Graduate School of Information Science Technology, The University of Tokyo, Tokyo, Japan

²Center for Advanced Intelligence Project (AIP), RIKEN, Tokyo, Japan

Abstract

Matrix reordering is a task to permute rows and columns of a given observed matrix so that the resulting reordered matrix shows some meaningful or interpretable structural patterns. Most of the existing matrix reordering techniques share a common process of extracting some feature representation from an observed matrix in some pre-defined way, and applying matrix reordering based on it. However, in some practical cases, we would not always have a prior knowledge about the structural pattern that an observed matrix has. In this paper, to address this problem, we propose a new matrix reordering method, Deep Two-way Matrix Reordering (DeepTMR), using a neural network model. The trained network can automatically extract nonlinear row/column features from an observed matrix, which can be used for matrix reordering. Moreover, and proposed DeepTMR provides us with the denoised mean matrix of a given observed matrix as an output of the trained network. Such a denoised mean matrix can be used for visualizing the global structure of the reordered observed matrix. We demonstrate the effectiveness of proposed DeepTMR by applying it to both synthetic and practical data sets.

Keywords: matrix reordering, relational data analysis, neural network, visualization

1 Introduction

Matrix reordering or seriation is a task to permute rows and columns of a given observed matrix so that the resulting matrix shows some meaningful or interpretable structural patterns [4, 22]. It has been shown that such reordering-based matrix visualization techniques enable us to capture the overview of various practical data matrices, including gene expression data [8, 12], document-term relationship data [5], and archaeological data [18] (e.g., relationships between tombs and objects in Egypt [26]). Particularly, in this paper, we focus on the two-mode two-way matrix reordering problem, where an observed matrix or *relational data matrix* $A \in \mathbb{R}^{n \times p}$ represents relationships between two generally different objects (e.g., rows for documents and columns for words) and the permutations of rows and columns are not required to be identical to each other, even if the row and column sizes are identical (i.e., $n = p$).

As discussed in [4], most of the matrix reordering techniques that have been proposed so far share a common process of extracting “intermediate objects” or feature representation from an observed matrix in some pre-defined way, and applying matrix reordering based on the extracted intermediate objects. For instance, in *biclustering-based* methods [25, 30], which is one of the seven categories defined in [4], we assume that an observed matrix consists of some homogeneous submatrices or *biclusters*, in each of which the entries are generated in i.i.d. sense. Based on such an assumption, we first estimate the locations (i.e., a set of row and column indices) of such biclusters, and then reorder the rows and columns of the original matrix according to the estimated bicluster structure. In this example, the intermediate objects correspond to the bicluster assignments of the rows and columns.

^{*}chihiro.watanabe@mist.i.u-tokyo.ac.jp

[†]taiji@mist.i.u-tokyo.ac.jp

However, in some practical cases, we would not always have prior knowledge about the structural pattern that a given observed matrix has, or there is no hint of what input features we should use as intermediate objects. In such cases, we need to try multiple methods and compare the results, in order to examine which method is suitable for analyzing the given observed matrix. Therefore, it would be desirable if the procedure of feature extraction from an observed matrix, as well as row/column reordering, can be automatically fitted to a given observed matrix.

In this paper, to address this problem, we propose a new matrix reordering method, Deep Two-way Matrix Reordering (DeepTMR), using a neural network model. Proposed DeepTMR consists of a neural network model that can be trained in an end-to-end manner, and the shallower part (i.e., encoder) of the trained network can automatically extract row/column features for matrix reordering based on a given observed matrix. The expressive power of a (deep) neural network model has been extensively studied in literature, including the well-known universal approximation theorems [9, 14, 19]. To exploit such flexibility of a neural network in the process of feature extraction, we transform the matrix reordering problem into parameter estimation of a neural network, which maps row and column input features to each entry value of an observed matrix. By using an autoencoder-like neural network architecture, we train proposed DeepTMR to extract one-dimensional row/column features from a given observed matrix so that each entry of observed matrix can be successfully reconstructed based on the extracted features. Then, the rows and columns are reordered based on the row/column features extracted by a trained network.

In the subsequent sections, we first refer to the existing matrix reordering methods and describe the difference between them and proposed DeepTMR in Section 2. Then, we explain how we perform two-way matrix reordering with proposed DeepTMR in Section 3. In Section 4, we experimentally show the effectiveness of proposed DeepTMR by applying it to both synthetic and practical data matrices. Finally, we discuss the results and the future works in Section 5, and conclude this paper in Section 6.

2 Existing works on matrix reordering

According to the recent survey [4], the matrix reordering algorithms can be roughly classified into seven categories: *Robinsonian*, *spectral*, *dimension-reduction*, *heuristic*, *graph-theoretic*, *biclustering*, and *interactive-user-controlled*. Among these categories, we refer to spectral and dimension-reduction ones, which include the methods based on singular value decomposition (SVD) [13, 24] and multidimensional scaling (MDS) [28, 29]. These methods are particularly relevant to proposed DeepTMR in that we assume some low-dimensional latent structure in an observed matrix. In Robinsonian and graph-theoretic methods, the general purpose is to find the optimal row/column orders for a given loss function [3, 7, 10, 27, 33]. Since to obtain the global optimal solution for such a combinatorial optimization problem gets infeasible with increasing matrix size, we need approximated algorithms for outputting local optimal solutions. For instance, it has been shown that the problem to find the optimal node reordering solution for a given arbitrary graph based on the bandwidth minimization or profile minimization is NP-hard [21, 23].

In spectral and dimension-reduction methods (and also proposed DeepTMR), instead of formulating matrix reordering as a combinatorial optimization problem, we assume that an observed matrix can be well approximated by some model with low-dimensional latent structure, estimate the parameter of the model, and interpret the estimation result as a feature for matrix reordering. By such formulation, we can avoid directly solving a combinatorial optimization problem on row/column reordering. It must be noted that biclustering-based methods are also based on such a low dimensionality assumption. However, unlike proposed DeepTMR and the dimension-reduction-based methods, they focus on detecting biclusters (i.e., a set of submatrices with coherent patterns) in an observed matrix, and the row/column orders within a bicluster is not considered in general, as also pointed out in [13].

Another advantage of the spectral and dimension-reduction methods over the other methods is that in some methods, including proposed DeepTMR, we can extract “denoised” mean information of a given observed matrix $A \in \mathbb{R}^{n \times p}$. When assuming that an observed matrix is generated from

some statistical model, the true purpose of matrix reordering is to reveal the row/column orders in the denoised mean matrix, not to maximize the similarities between adjacent rows/columns in the original data matrix with noise. The spectral and dimension-reduction methods address this problem, while the Robinsonian and graph-theoretic methods do not. Particularly, in the following examples, the SVD-based method [24] (and also proposed DeepTMR) provide us with a denoised mean matrix of a given relational data matrix. For instance, in the method of [24], we derive a rank-one approximation of the original matrix $A = \mathbf{r}\mathbf{c}^\top$, where $\mathbf{r} \in \mathbb{R}^n$ and $\mathbf{c} \in \mathbb{R}^p$. In this case, we can expect that the approximated observed matrix $\mathbf{r}\mathbf{c}^\top$ preserves a global structure of the original matrix A , whereas the noise in each entry is removed. Such a denoised mean matrix can be used for visualizing the global structure of an observed matrix, together with the reordered data matrix.

In the following two paragraphs, We refer to the basic matrix reordering methods based on singular value decomposition and multidimensional scaling. Each of these methods is based on a specific assumption on low-dimensionality of an observed matrix. The main advantages of proposed DeepTMR to these conventional methods are as follows:

- Proposed DeepTMR can extract a low-dimensional row/column features from an observed matrix more flexibly than the other methods. Unlike SVD-based methods, proposed DeepTMR can be applied without the bilinear assumption. Moreover, unlike MDS, it does not require to specify a distance function in advance for representing the relationships (i.e., proximity) between a pair of rows/columns appropriately. The row/column encoder of proposed DeepTMR, which applies a nonlinear mapping from a row/column to a one-dimensional feature, is automatically obtained by training a neural network model.
- Unlike MDS, proposed DeepTMR can provide us with the denoised mean matrix of a given observed matrix, as well as the row/column orders. Such a denoised mean matrix can be obtained as an output of the trained neural network, and it can be used for visualizing the global structure of the reordered observed matrix.

Singular Value Decomposition (SVD) - (1) Rank-one approximation (SVD-Rank-One)
Several studies have proposed to utilize SVD for matrix reordering [13, 24]. In [24], for instance, Liu et al. have proposed to model an $n \times p$ observed matrix A with the following bilinear form:

$$\begin{aligned} \mathbf{r} &= (r_i)_{1 \leq i \leq n}, \quad \mathbf{c} = (c_j)_{1 \leq j \leq p}, \quad E = (E_{ij})_{1 \leq i \leq n, 1 \leq j \leq p}, \\ A &= \mathbf{r}\mathbf{c}^\top + E, \end{aligned} \tag{1}$$

where \mathbf{r} and \mathbf{c} , respectively, are the parameters corresponding to the rows and columns, and E is a residual matrix. Based on the above model, we estimate the parameters \mathbf{r} and \mathbf{c} as follows:

$$\begin{aligned} \boldsymbol{\theta} &\equiv [r_1 \quad \cdots \quad r_n \quad c_1 \quad \cdots \quad c_p]^\top, \\ \hat{\boldsymbol{\theta}} &= \arg \min_{\boldsymbol{\theta} \in \mathbb{R}^{n+p}} \|A - \mathbf{r}\mathbf{c}^\top\|_F^2. \end{aligned} \tag{2}$$

It can be proven that an optimal solution of (2) is given by $\hat{\mathbf{r}} = \sqrt{\lambda_1} \mathbf{u}_1$ and $\hat{\mathbf{c}} = \sqrt{\lambda_1} \mathbf{v}_1$, where λ_1 is the largest singular value of matrix A and $\mathbf{u}_1 \in \mathbb{R}^n$ and $\mathbf{v}_1 \in \mathbb{R}^p$, respectively, are the corresponding row and column singular vectors. Based on this fact, the order of the estimated row and column parameters, $\hat{\mathbf{r}}$ and $\hat{\mathbf{c}}$, respectively, can be used for matrix reordering.

Singular Value Decomposition (SVD) - (2) Angle between the top two singular vectors (SVD-Angle) Friendly has pointed out that the structure of a given data matrix cannot always be represented sufficiently by a single principal component and has proposed to define the row/column orders using the angle between the top two singular vectors [13]. In the method proposed in [13], an

observed matrix A is first mean-centered and scaled as follows:

$$\begin{aligned}\tilde{A}^{(0)} &= (\tilde{A}_{ij}^{(0)})_{1 \leq i \leq n, 1 \leq j \leq p}, \quad \tilde{A}_{ij}^{(0)} = A_{ij} - \frac{1}{p} \sum_{j=1}^p A_{ij}, \\ \tilde{A} &= (\tilde{A}_{ij})_{1 \leq i \leq n, 1 \leq j \leq p}, \quad \tilde{A}_{ij} = \frac{\tilde{A}_{ij}^{(0)}}{\sqrt{\frac{1}{p} \sum_{j=1}^p (\tilde{A}_{ij}^{(0)})^2}}.\end{aligned}\quad (3)$$

Let \mathbf{u}_i be the row singular vector of the scaled observed matrix \tilde{A} which corresponds to the i th largest singular value. The angle α_i between the top two row singular vectors is given by

$$\alpha_i = \tan^{-1}(u_{i2}/u_{i1}) + \pi I[u_{i1} \leq 0], \quad (4)$$

where $I[\cdot]$ is an indicator function. The row order is determined by splitting the angles $\{\alpha_i\}$ at the largest gap between two adjacent angles. The column order can be defined in the same way as the row one, by replacing the observed matrix \tilde{A} with the transposed matrix \tilde{A}^\top .

Multidimensional Scaling (MDS) MDS is also a dimension reduction method that can be used for matrix reordering [28, 29]. In MDS, we use a proximity matrix, each of whose entry represents a distance between a pair of rows or columns. For instance, we can define a proximity matrix D for rows based on a given observed matrix $A \in \mathbb{R}^{n \times p}$ as follows:

$$D = (D_{ii'})_{1 \leq i, i' \leq n}, \quad D_{ii'} = \left(\sum_{j=1}^n (A_{ij} - A_{i'j})^2 \right)^{\frac{1}{2}}, \quad i, i' = 1, \dots, n. \quad (5)$$

The purpose of MDS is to obtain k -dimensional representation $\tilde{A} \in \mathbb{R}^{n \times k}$ of the original observed matrix A based on matrix D , where $k \leq n, p$. First, we define the following matrices:

$$\begin{aligned}\tilde{D} &= (\tilde{D}_{ii'})_{1 \leq i, i' \leq n}, \quad \tilde{D}_{ii'} = D_{ii'}^2, \quad i, i' = 1, \dots, n, \\ Q &= (Q_{ii'})_{1 \leq i, i' \leq n}, \quad Q_{ii'} = 1, \quad i, i' = 1, \dots, n, \\ B &= -\frac{1}{2} (I - n^{-1}Q) \tilde{D} (I - n^{-1}Q).\end{aligned}\quad (6)$$

It can be easily shown that B is a semi-positive definite matrix. Let λ_i and \mathbf{v}_i , respectively, be the i th largest eigenvalue of matrix B and the corresponding eigenvector. The k -dimensional representation \tilde{A} of matrix A is given by

$$\tilde{A} = [\mathbf{v}_1 \ \cdots \ \mathbf{v}_k] \text{diag}(\sqrt{\lambda_1}, \dots, \sqrt{\lambda_k}). \quad (7)$$

It has been proven that the above solution \tilde{A} minimizes the *Strain*, which is given by $\mathcal{L}(\tilde{A}) = \|\tilde{A}\tilde{A}^\top - B\|_F^2$ [6]. By setting $k = 1$, we can obtain one-dimensional row feature of observed matrix A , which can be used for determining the row order. The column order can be defined in the same way as the row one, by replacing the observed matrix A with the transposed matrix A^\top .

3 Deep Two-way Matrix Reordering

Given an $n \times p$ observed matrix $A \in \mathbb{R}^{n \times p}$, our purpose is to reorder the row and column indices of matrix A so that the resulting matrix \underline{A} shows some structure (e.g., block structure), as shown in Figure 1.

The entire network architecture of proposed DeepTMR is shown in Figure 2. To extract the row and column feature of a given matrix A , we propose a new neural network model DeepTMR that

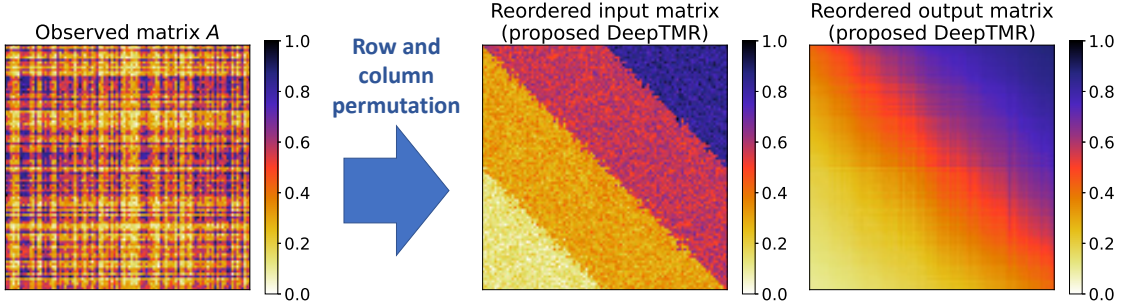


Figure 1: Matrix reordering problem. Given an observed matrix A (left), proposed DeepTMR reorders the rows and columns of matrix A so that the reordered input matrix (center) shows some meaningful or interpretable structure. Proposed DeepTMR provides us with the denoised mean matrix of the reordered matrix (right) as output of a trained network, as well as the row/column orderings.

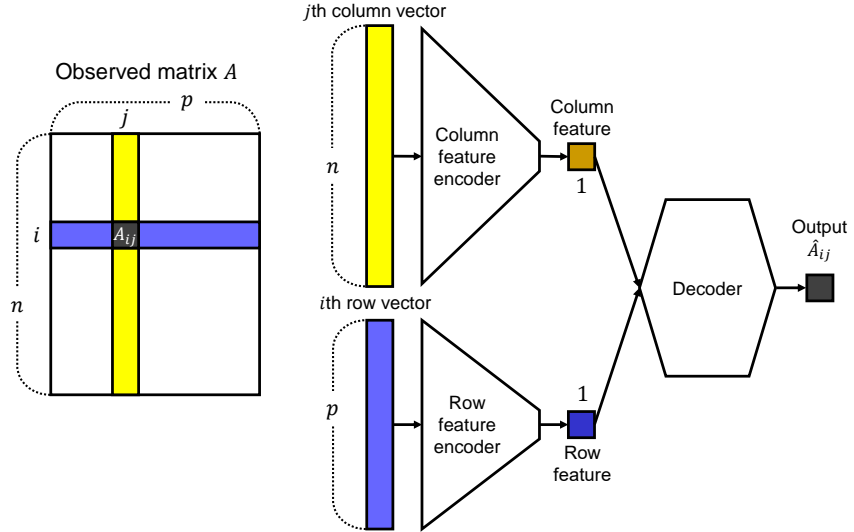


Figure 2: Model architecture of proposed DeepTMR. Given an observed matrix A , DeepTMR is trained to reconstruct each entry A_{ij} from one-dimensional row and column features, which are extracted from the i th row and the j th column of matrix A . After training the network, we reorder the rows and columns of matrix A based on the row and column features extracted in the middle layer.

has an autoencoder-like architecture. In DeepTMR, the (i, j) th entry A_{ij} of the observed matrix A is estimated based on its row and column data vectors, $\mathbf{r}^{(i)}$ and $\mathbf{c}^{(j)}$, respectively, which are given by

$$\begin{aligned}\mathbf{r}^{(i)} &= (r_{j'}^{(i)})_{1 \leq j' \leq p}, & r_{j'}^{(i)} &= A_{ij'}, \\ \mathbf{c}^{(j)} &= (c_{i'}^{(j)})_{1 \leq i' \leq n}, & c_{i'}^{(j)} &= A_{i'j}.\end{aligned}\quad (8)$$

Then, from these input data vectors, the feature of the i th row and the j th column, g_i and h_j , respectively, are extracted by row and column encoder networks:

$$g_i = \text{ROWENC}(\mathbf{r}^{(i)}), \quad (9)$$

$$h_j = \text{COLUMNENC}(\mathbf{c}^{(j)}). \quad (10)$$

Here, $\text{ROWENC} : \mathbb{R}^p \mapsto \mathbb{R}$ and $\text{COLUMNENC}(\cdot) : \mathbb{R}^n \mapsto \mathbb{R}$ can be implemented as arbitrary neural network architectures, as long as they have fixed numbers of units, m and \tilde{m} , respectively, in the input and output layers [i.e., $(m, \tilde{m}) = (p, 1)$ for $\text{ROWENC}(\cdot)$ and $(m, \tilde{m}) = (n, 1)$ for $\text{COLUMNENC}(\cdot)$].

From these row and column features, the (i, j) th entry A_{ij} is estimated by using a decoder network:

$$\hat{A}_{ij} = \text{DEC}(g_i, h_j), \quad (11)$$

where $\text{DEC} : \mathbb{R}^2 \mapsto \mathbb{R}$ can be implemented as an arbitrary neural network architecture with two input layer units and one output layer unit.

By using mini-batch learning, the entire network is trained so that the following mean squared error with L_2 regularization term is minimized:

$$\mathcal{L} = \frac{1}{|\mathcal{I}_t|} \sum_{(i,j) \in \mathcal{I}_t} (A_{ij} - \hat{A}_{ij})^2 + \lambda \|\mathbf{w}\|_2, \quad (12)$$

where \mathcal{I}_t is a set of row and column indices (i, j) in a mini-batch of the t th iteration, λ is a hyperparameter, and \mathbf{w} is a vector of parameters in the entire network¹.

Finally, we define matrix \underline{A} with reordered rows and columns. By using the trained row and column encoder networks, we define the following two feature vectors:

$$\begin{aligned}\mathbf{g} &= [\text{ROWENC}(\mathbf{r}^{(1)}) \ \dots \ \text{ROWENC}(\mathbf{r}^{(n)})]^\top, \\ \mathbf{h} &= [\text{COLUMNENC}(\mathbf{c}^{(1)}) \ \dots \ \text{COLUMNENC}(\mathbf{c}^{(p)})]^\top.\end{aligned}\quad (13)$$

Since the network has been trained to recover each entry value only from the corresponding row and column data vectors, vectors \mathbf{g} and \mathbf{h} can be expected to reflect the row and column features of the original matrix A . Based on this conjecture, we define π^{row} as a permutation of $\{1, 2, \dots, n\}$ that represents the ascending order of the entries of \mathbf{g} (i.e., $g_{\pi^{\text{row}}(1)} \leq g_{\pi^{\text{row}}(2)} \leq \dots \leq g_{\pi^{\text{row}}(n)}$ holds). Similarly, we define π^{column} as a permutation of $\{1, 2, \dots, p\}$ that represents the ascending order of the entries of \mathbf{h} (i.e., $h_{\pi^{\text{column}}(1)} \leq h_{\pi^{\text{column}}(2)} \leq \dots \leq h_{\pi^{\text{column}}(p)}$ holds). By using these row and column permutations, we obtain the reordered row and column features, $\underline{\mathbf{g}}$ and $\underline{\mathbf{h}}$, respectively, and the reordered observed and estimated matrices, \underline{A} and \hat{A} , respectively, as follows:

$$\begin{aligned}\underline{\mathbf{g}} &= (\underline{g}_i)_{1 \leq i \leq n}, & \underline{g}_i &= g_{\pi^{\text{row}}(i)}, \\ \underline{\mathbf{h}} &= (\underline{h}_j)_{1 \leq j \leq p}, & \underline{h}_j &= h_{\pi^{\text{column}}(j)}, \\ \underline{A} &= (\underline{A}_{ij})_{1 \leq i \leq n, 1 \leq j \leq p}, & \underline{A}_{ij} &= A_{\pi^{\text{row}}(i)\pi^{\text{column}}(j)}, \\ \hat{\underline{A}} &= (\hat{\underline{A}}_{ij})_{1 \leq i \leq n, 1 \leq j \leq p}, & \hat{\underline{A}}_{ij} &= \hat{A}_{\pi^{\text{row}}(i)\pi^{\text{column}}(j)}.\end{aligned}\quad (14)$$

¹In the experiments in Section 4, we defined \mathbf{w} as a vector of all the weights and biases in the linear layers of encoder and decoder networks.

4 Experiments

To check the effectiveness of proposed DeepTMR, we applied it to both synthetic and practical relational data matrices and plotted their latent row-column structures obtained by the DeepTMR. For all the experiments,

- We initialized the weights and biases of the linear layers using the method described in [15]. That is, each weight value that connects the l th and $(l+1)$ th layers is initialized based on a uniform distribution on the interval $[-1/\sqrt{m^{(l)}}, 1/\sqrt{m^{(l)}}]$, where $m^{(l)}$ is the number of units in the l th layer. As for the biases, we set their initial values at zero.
- We used Adam optimizer [20] with $\beta_1 = 0.9$, $\beta_2 = 0.999$, and $\epsilon = 1.0 \times 10^{-8}$ for training proposed DeepTMR network².

4.1 Preliminary experiment using synthetic data sets

First, we generated three types of synthetic data sets with latent row and column structures, applied proposed DeepTMR, and checked if we could successfully recover the latent structure of given observed matrices. For all the following three models, we set the matrix size at $(n, p) = (100, 100)$.

Latent block model First, we generated a matrix based on a latent block model (LBM) [2, 16, 17]. In an LBM, we assume that each row and column of a given matrix $\bar{A}^{(0)} \in \mathbb{R}^{n \times p}$ belong to one of the K row clusters and H column clusters, respectively. Let c_i and d_j , respectively, be the row cluster index of the i th row and the column cluster index of the j th column of matrix $\bar{A}^{(0)}$. In this experiment, we set the number of row and column clusters at $(K, H) = (3, 3)$, and define the row and column cluster assignments as follows:

$$\begin{aligned} n^{(0)} &= \text{ceil}\left(\frac{n}{K}\right), \quad p^{(0)} = \text{ceil}\left(\frac{p}{H}\right), \\ c_1 &= \dots = c_{n^{(0)}} = 1, \quad c_{n^{(0)}+1} = \dots = c_{2n^{(0)}} = 2, \quad \dots, \quad c_{(K-1)n^{(0)}+1} = \dots = c_n = K, \\ d_1 &= \dots = d_{p^{(0)}} = 1, \quad d_{p^{(0)}+1} = \dots = d_{2p^{(0)}} = 2, \quad \dots, \quad d_{(H-1)p^{(0)}+1} = \dots = d_p = H, \end{aligned} \quad (15)$$

where $\text{ceil}(\cdot)$ is the ceiling function. Based on the above definitions, in an LBM, we assume that each entry of matrix $\bar{A}^{(0)}$ is independently generated from a block-wise identical distribution. Specifically, we generated each (i, j) th entry $\bar{A}_{ij}^{(0)}$ based on a Gaussian distribution with mean $B_{c_i d_j}$ and standard deviation σ , which were given by

$$B = \begin{bmatrix} 0.9 & 0.4 & 0.8 \\ 0.1 & 0.6 & 0.2 \\ 0.5 & 0.3 & 0.7 \end{bmatrix}, \quad \sigma = 0.05. \quad (16)$$

Striped pattern model To show that proposed DeepTMR can reveal latent row-column structure that is not necessarily represented as a set of rectangular blocks, we also tried the striped pattern model (SPM). An SPM is similar to an LBM in that we assume that each entry of a given matrix $\bar{A}^{(0)} \in \mathbb{R}^{n \times p}$ belongs to one of the K clusters and that it is independently generated from a cluster-wise identical distribution. However, unlike an LBM, in an SPM, we assume that the cluster assignments show a striped pattern, not a regular grid pattern. Specifically, let c_{ij} be the cluster index of the

²As for learning rates η , we used different settings in each experiment, as shown in Table 1

Table 1: Experimental settings of learning rate η , number of epochs T (the total number of iterations is given by $\text{ceil}[Tnp/|\mathcal{I}|]$), regularization hyperparameter λ , number of sets of row and column indices in a mini-batch $|\mathcal{I}|$, and number of units in ROWENC, COLUMNENC, and DEC networks, $\mathbf{m}^{\text{ROWENC}}$, $\mathbf{m}^{\text{COLUMNENC}}$, and \mathbf{m}^{DEC} , respectively (from input to output).

	η	T	λ	$ \mathcal{I} $	$\mathbf{m}^{\text{ROWENC}}$	$\mathbf{m}^{\text{COLUMNENC}}$	\mathbf{m}^{DEC}				
Sec. 4.1, LBM	1.0×10^{-2}	1×10^2	1.0×10^{-10}	2×10^2	$[p, 10, 1]$	$[n, 10, 1]$	$[2, 10, 1]$				
Sec. 4.1, SPM											
Sec. 4.1, GBM											
Sec. 4.2, DGM		2×10^2									
Sec. 4.3		5×10^2									
Sec. 4.4								1×10^2			

(i, j) th entry $\bar{A}_{ij}^{(0)}$ of matrix $\bar{A}^{(0)}$. In an SPM, the cluster assignment is given by

$$\begin{aligned} n^{(0)} &= \text{ceil} \left(\frac{n+p}{K} \right), \\ c_{ij} &= \text{floor} \left(\frac{i+j-2}{n^{(0)}} \right) + 1, \quad i = 1, \dots, n, \quad j = 1, \dots, p. \end{aligned} \quad (17)$$

Based on the above cluster assignments with a striped pattern, we generated each (i, j) th entry $\bar{A}_{ij}^{(0)}$ of matrix $\bar{A}^{(0)}$ based on a Gaussian distribution with mean $b_{c_{ij}}$ and standard deviation σ , which were given by

$$\mathbf{b} = [0.9 \quad 0.6 \quad 0.3 \quad 0.1], \quad \sigma = 0.05. \quad (18)$$

Gradation block model In the above LBM and SPM, we assume that each entry is generated from a cluster-wise identical distribution. In gradation block model (GBM), we consider a different case from these models, where a matrix $\bar{A}^{(0)} \in \mathbb{R}^{n \times p}$ contains a block or submatrix with a gradation (i.e., continuous) pattern. Specifically, let I and J , respectively, be the sets of row and column indices that belongs to the block with a gradation pattern. We assume that the (i, j) th entry $\bar{A}_{ij}^{(0)}$ of matrix $\bar{A}^{(0)}$ is generated from a Gaussian distribution with mean B_{ij} and standard deviation σ , which were given by

$$\begin{aligned} n^{(0)} &= \text{ceil} \left(\frac{n}{2} \right), \quad p^{(0)} = \text{ceil} \left(\frac{p}{2} \right), \\ B_{ij} &= \begin{cases} 0.1 & \text{if } (i > n^{(0)}) \cup (j > p^{(0)}), \\ \frac{0.8(j-1)}{p^{(0)}-1} + 0.1 & \text{if } (i \leq n^{(0)}) \cap (j \leq p^{(0)}), \end{cases} \quad i = 1, \dots, n, \quad j = 1, \dots, p, \\ \sigma &= 0.05. \end{aligned} \quad (19)$$

For all the above three models, once we generated matrix $\bar{A}^{(0)}$, we define matrix \bar{A} as follows:

$$\bar{A} = (\bar{A}_{ij})_{1 \leq i \leq n, 1 \leq j \leq p}, \quad \bar{A}_{ij} = \frac{\bar{A}_{ij}^{(0)} - \min_{(i,j)=(1,1), \dots, (n,p)} \bar{A}_{ij}^{(0)}}{\max_{(i,j)=(1,1), \dots, (n,p)} \bar{A}_{ij}^{(0)} - \min_{(i,j)=(1,1), \dots, (n,p)} \bar{A}_{ij}^{(0)}}. \quad (20)$$

By definition, the maximum and minimum entries of matrix \bar{A} are one and zero, respectively. Then, we applied random permutation to the rows and columns of matrix \bar{A} to obtain an observed matrix A . Finally, we applied proposed DeepTMR to the observed matrix A , and checked if it could recover the latent row-column structure of matrix A . The hyperparameter settings for training proposed DeepTMR are given in Table 1.

Figures 3, 4, and 5, show the results of LBM, SPM, and GBM, respectively. For each figure, we plotted matrix \bar{A} , observed matrix A , reordered observed and estimated matrices, \underline{A} and \hat{A} , respectively, row and column feature vectors, \mathbf{g} and \mathbf{h} , respectively, and their reordered versions $\underline{\mathbf{g}}$ and $\underline{\mathbf{h}}$. From the figures of the reordered matrices \underline{A} and \hat{A} , we see that proposed DeepTMR could successfully extract the latent row-column structures (i.e., block structure, striped pattern, and gradation block structure) of given observed matrices. Particularly, the figures of the reordered output matrices \hat{A} show that the outputs of the DeepTMR network reflect the global structures of given observed matrices. It must be noted that the order of the row and column indices in matrices \underline{A} and \hat{A} to represent the latent structure is not always unique and thus it is not necessarily identical with that of the original matrix A , as shown in these figures. For instance, the latent structures of the three models (i.e., LBM, SPM, and GBM) can be represented also by flipping or reversing the order of row or column indices. Moreover, for an LBM, arbitrary orders of the row or column clusters are permitted in representing the latent block structure.

From the figures of the vectors $\underline{\mathbf{g}}$ and $\underline{\mathbf{h}}$, we see that they captured the one-dimensional feature of each row and column. For example, in the LBM case of Figure 3, the row (column) feature values in the same row (column) cluster are more similar to each other, compared to those in the mutually different row (column) clusters. In the GBM case of Figure 5, we see that the row features are divided to two groups, one of which contains the gradation pattern block and the other of which does not. As for the column features, its value increases continuously within the gradation pattern block, whereas the remaining feature values are almost constant.

4.2 Comparison to the existing matrix reordering methods

We also conducted a quantitative comparison between proposed DeepTMR and the existing matrix reordering methods that we introduced in Section 2. As comparison targets, we chose the spectral/dimension-reduction methods based on SVD-Rank-One, SVD-Angle, and MDS, whose specific algorithms are described in Section 2. For quantitative evaluation of these methods, we generated synthetic data matrices with true row/column orders, applied the proposed and conventional methods to them, and compared the accuracy in matrix reordering. For simplicity, we consider the following data matrices, whose true row/column orders can be represented uniquely, except for row/column flipping.

Diagonal gradation model We generated a matrix $\bar{A}^{(0)} \in \mathbb{R}^{n \times p}$ with the following diagonal gradation pattern, where we set the matrix size at $(n, p) = (100, 100)$. We assume that the (i, j) th entry $\bar{A}_{ij}^{(0)}$ of matrix $\bar{A}^{(0)}$ is generated from a Gaussian distribution with mean B_{ij} , which was given by

$$B_{ij} = 0.9 - 0.8 \frac{|i - j|}{\max\{n, p\}}, \quad i = 1, \dots, n, \quad j = 1, \dots, p. \quad (21)$$

As for the standard deviation, we tried the following ten settings: $\sigma_t = 0.03t$ for $t = 1, \dots, 10$. As in Section 4.1, we defined matrix \bar{A} using matrix $\bar{A}^{(0)}$ based on (20), and applied random permutation to the rows and columns of matrix \bar{A} to obtain an observed matrix A . For each setting of t , we generated 10 observed matrices and applied proposed DeepTMR, SVD-Rank-One, SVD-Angle, and MDS to them. Since the training result of proposed DeepTMR depends on its initial parameters and the selection of mini-batch in each iteration, for the same observed matrix A , we tried training of the DeepTMR model five times, and adopt the trained model with the minimum mean training loss for the last 100 iterations. The other hyperparameter settings for training proposed DeepTMR are given in Table 1.

To quantitatively evaluate these methods, we computed the following matrix reordering error. Let $P \in \mathbb{R}^{n \times p}$ and $\bar{P} \in \mathbb{R}^{n \times p}$ be the mean matrices, whose (i, j) th entry is the (population) mean of A_{ij} and \bar{A}_{ij} , respectively. Let $\pi^{\text{row}(0)}$ and $\pi^{\text{column}(0)}$, respectively, be the permutations of $\{1, 2, \dots, n\}$ and $\{1, 2, \dots, p\}$, which indicate the orders of rows and columns determined by each method. We

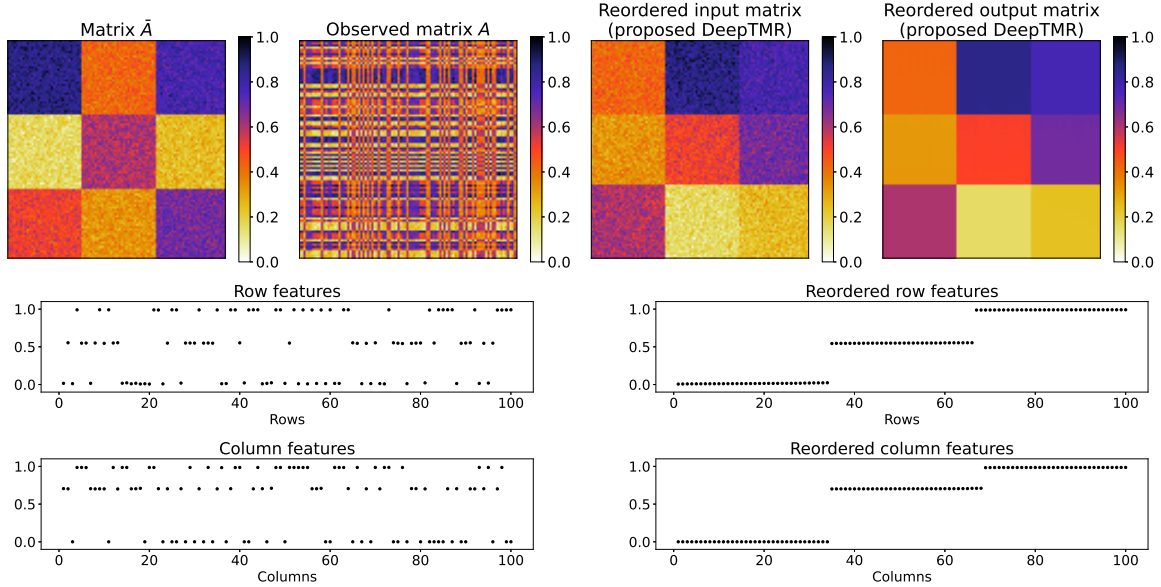


Figure 3: Results of the **LBM**. Top figures: original matrix \bar{A} , observed matrix A obtained by applying random row-column permutation to \bar{A} , reordered input matrix \hat{A} , and reordered output matrix \hat{A} (left to right). Bottom figures: Encoded row and column features \mathbf{g} and \mathbf{h} and the reordered row and column features $\underline{\mathbf{g}}$ and $\underline{\mathbf{h}}$ (left to right).

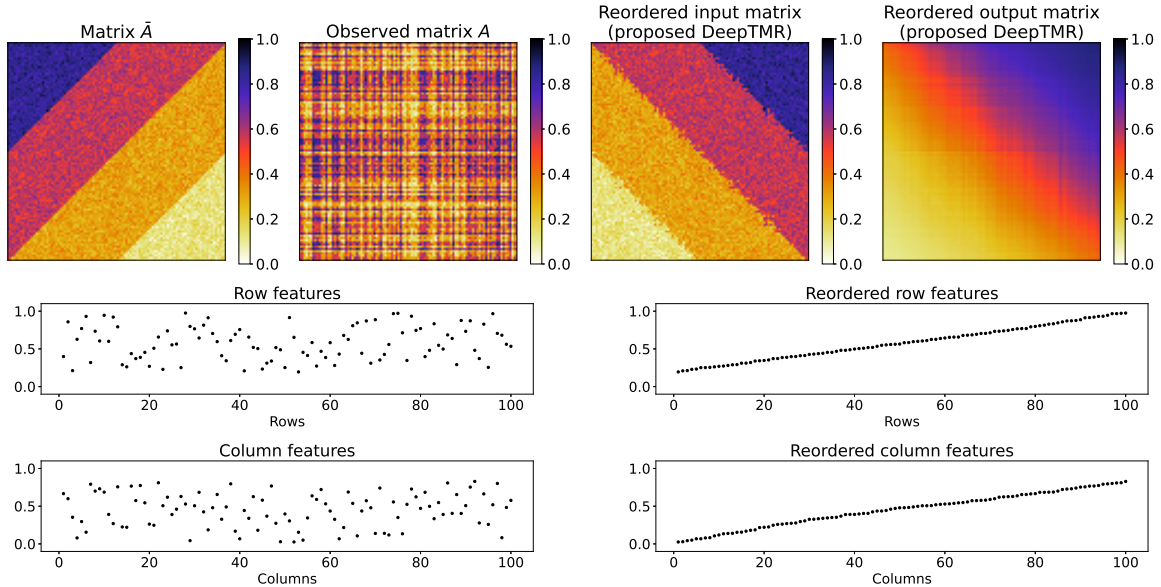


Figure 4: Results of the **striped pattern model**. Matrices \bar{A} , A , \hat{A} , and \hat{A} and vectors \mathbf{g} , \mathbf{h} , $\hat{\mathbf{g}}$, $\hat{\mathbf{h}}$.

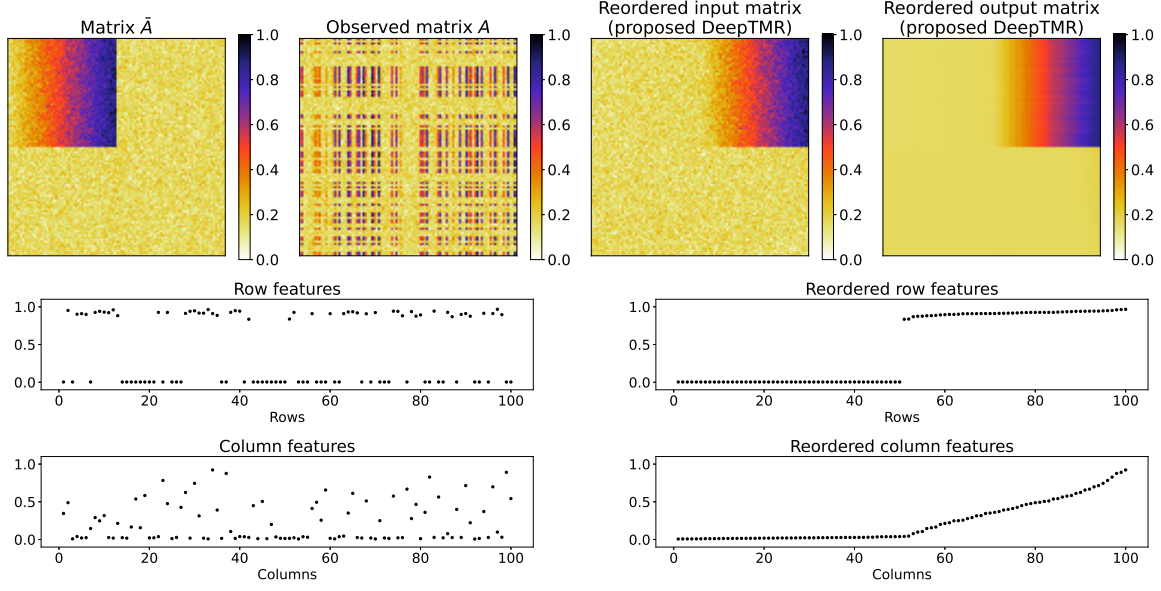


Figure 5: Results of the **gradation block model**. Matrices \bar{A} , A , \underline{A} , \hat{A} and vectors \mathbf{g} , \mathbf{h} , $\underline{\mathbf{g}}$, $\underline{\mathbf{h}}$.

define the flipped versions of these orders as $\pi^{\text{row}(1)}$ and $\pi^{\text{column}(1)}$ (i.e., $\pi^{\text{row}(0)}(i) = \pi^{\text{row}(1)}(n - i + 1)$ and $\pi^{\text{column}(0)}(j) = \pi^{\text{column}(1)}(p - j + 1)$ for $i = 1, \dots, n$ and $j = 1, \dots, p$). Let $\bar{\pi}^{\text{row}}$ and $\bar{\pi}^{\text{column}}$, respectively, be the orders of rows and columns which reconstruct the original (correctly ordered) matrix \bar{A} . Remark that both $\pi^{\text{row}(0)} = \bar{\pi}^{\text{row}}$ and $\pi^{\text{row}(1)} = \bar{\pi}^{\text{row}}$ indicate that the correct row ordering is obtained. Based on this fact, we re-define the row/column orders π^{row} and π^{column} obtained by each method as follows:

$$(\hat{k}, \hat{h}) = \arg \min_{(k, h) \in \{(0,0), (0,1), (1,0), (1,1)\}} \frac{1}{np} \sum_{i=1}^n \sum_{j=1}^p (\bar{P}_{ij} - P_{\pi^{\text{row}(k)}(i) \pi^{\text{column}(h)}(j)})^2, \\ \pi^{\text{row}} = \pi^{\text{row}(\hat{k})}, \quad \pi^{\text{column}} = \pi^{\text{column}(\hat{h})}. \quad (22)$$

Finally, we define the matrix reordering error E as follows:

$$E = \frac{1}{np} \sum_{i=1}^n \sum_{j=1}^p (\bar{P}_{ij} - P_{\pi^{\text{row}}(i) \pi^{\text{column}}(j)})^2. \quad (23)$$

Figures 6 and 7, respectively, show the examples of matrices \bar{A} and A with different levels of noise standard deviation σ_t , where $t = 1, \dots, 10$. Figures 8, 9, 10, and 11, respectively, show the examples of the reordered observed matrix \underline{A} based on the row/column orderings $(\pi^{\text{row}}, \pi^{\text{column}})$ obtained by proposed DeepTMR, SVD-Rank-One, SVD-Angle, and MDS. Figure 12 shows the reordered output matrix \hat{A} of proposed DeepTMR. From these figures, we see that proposed DeepTMR and MDS could relatively successfully reorder the observed matrix, compared to the SVD-based methods. Figure 13 shows the matrix reordering error of proposed DeepTMR, SVD-Rank-One, SVD-Angle, and MDS. This figure shows that proposed DeepTMR could achieve the minimum matrix reordering error in this setting, compared to the other three methods.

4.3 Experiment using Divorce Predictors data set

Next, we applied proposed DeepTMR to Divorce Predictors data set [31, 32] from UCI Machine Learning Repository [11]. The original data matrix $A^{(0)}$ consists of 170 rows and 54 columns, which

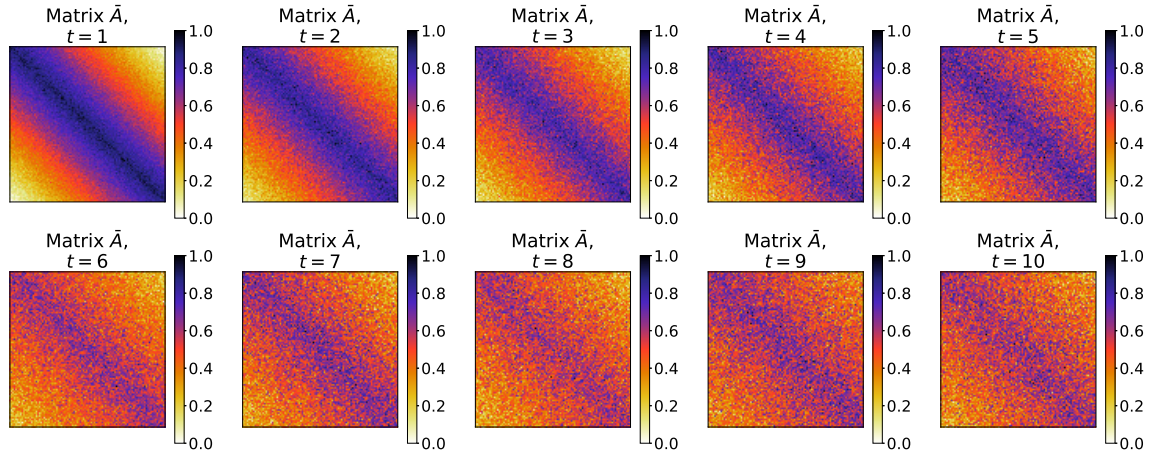


Figure 6: Examples of matrix \bar{A} of **diagonal gradation model** with different levels of noise standard deviation.

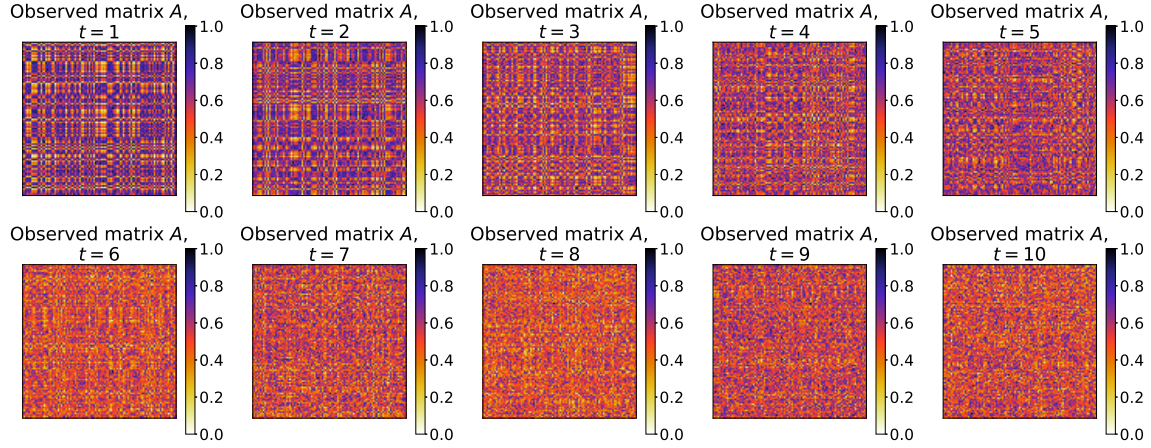


Figure 7: Examples of observed matrix A of **diagonal gradation model** with different levels of noise standard deviation.

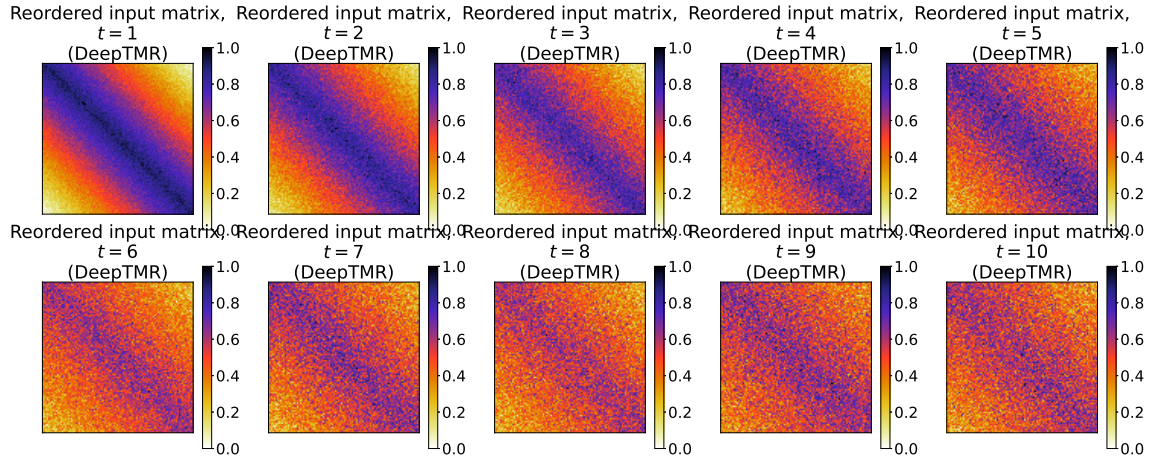


Figure 8: Examples of reordered input matrix A of **diagonal gradation model** with different levels of noise standard deviation (**DeepTMR**).

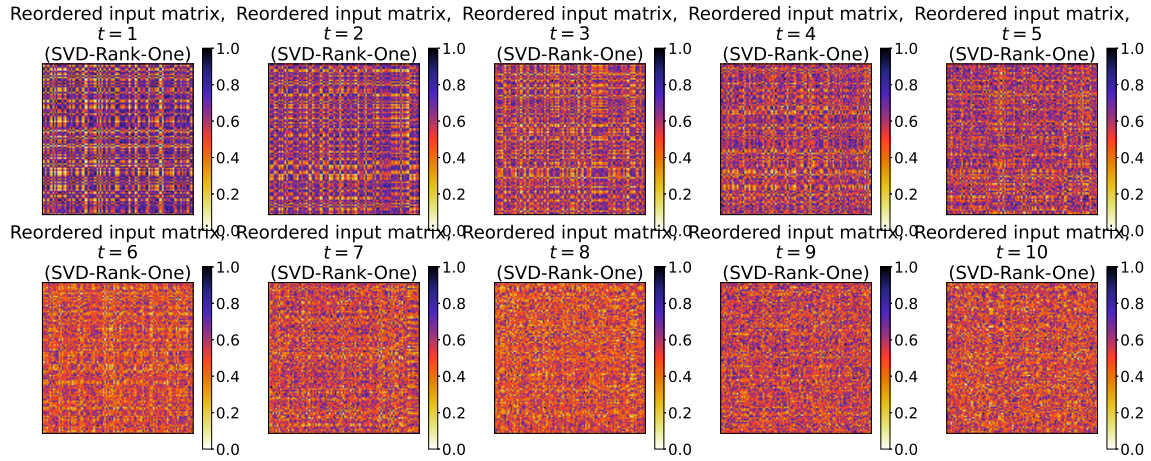


Figure 9: Examples of reordered input matrix \underline{A} of **diagonal gradation model** with different levels of noise standard deviation (**SVD-Rank-One**).

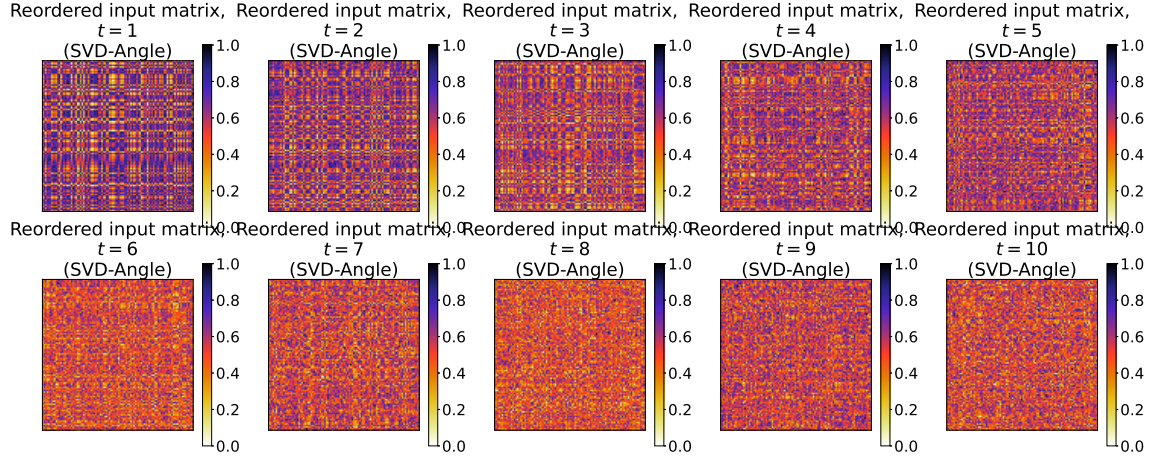


Figure 10: Examples of reordered input matrix \underline{A} of **diagonal gradation model** with different levels of noise standard deviation (**SVD-Angle**).

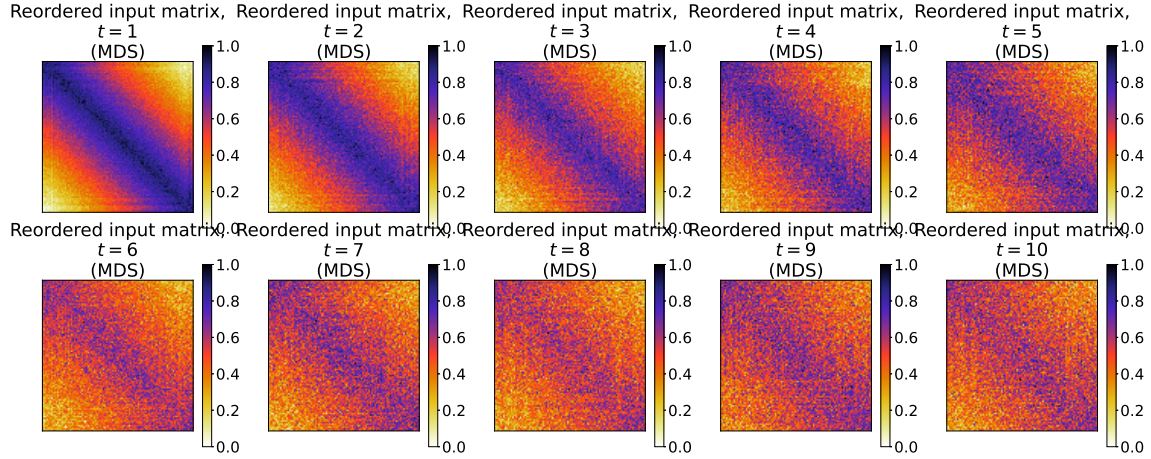


Figure 11: Examples of reordered input matrix \underline{A} of **diagonal gradation model** with different levels of noise standard deviation (**MDS**).

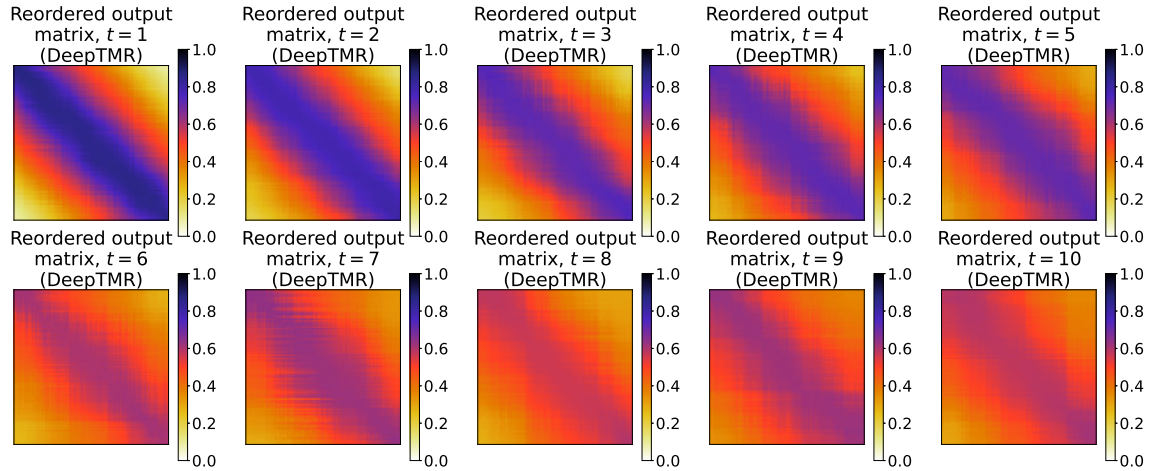


Figure 12: Examples of reordered output matrix \hat{A} of **diagonal gradation model** with different levels of noise standard deviation (**DeepTMR**).

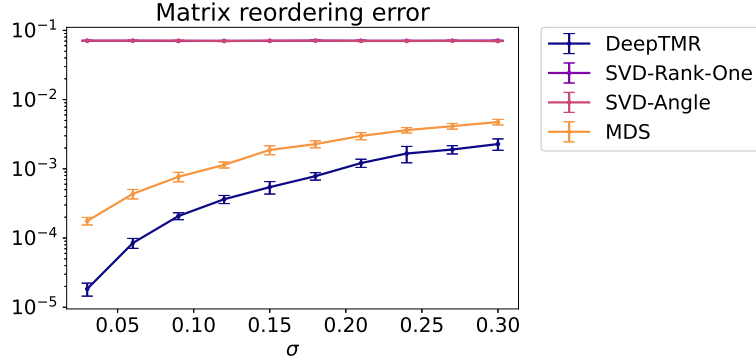


Figure 13: Matrix reordering error of proposed DeepTMR, SVD-Rank-One, SVD-Angle, and MDS. The error bars indicate the sample standard deviations of the results for ten trials.

represent the participants of a questionnaire and the attributes, respectively. Each entry $A_{ij}^{(0)} \in \{0, 1, \dots, 4\}$ shows the Divorce Predictors Scale (DPS), the higher value of which indicates higher divorce risk. The meaning of five-factor scale is as follows: 0 for “Never,” 1 for “Rarely,” 2 for “Occasionally,” 3 for “Often,” and 4 for “Always,” for Attributes 31 to 54, while it is reversed (i.e., 0 for “Always” and 4 for “Never”) for Attributes 1 to 30. The meaning of each attribute index of this data set is given in Appendix A.

As in Section 4.1, we define observed matrix A based on (20) by replacing $\bar{A}^{(0)}$ and \bar{A} with $A^{(0)}$ and A , respectively. Then, we applied proposed DeepTMR to the observed matrix A , and checked the latent row-column structure of matrix A that was extracted by the DeepTMR. The hyperparameter settings for training proposed DeepTMR are given in Table 1.

Figure 14 shows the results of matrices A , \underline{A} , \hat{A} and vectors \mathbf{g} , \mathbf{h} , $\underline{\mathbf{g}}$, $\underline{\mathbf{h}}$ for this data set. For each row in matrices A , \underline{A} , and \hat{A} , the class label of “divorced” or “married” are shown in different colors at the left side of the matrix. From the reordered input and output matrices \underline{A} and \hat{A} , respectively, we see the latent row-column structure of the observed matrix. Roughly, the DPS takes higher value in “divorced” rows than in “married” ones. However, some divorced participants show relatively low DPS in some attributes (e.g., Attributes 21, 22, and 28). We also see that both divorced and married participants

show relatively high DPS in Attributes 43 and 48, whereas most participants show relatively low DPS in Attributes 6 and 7, both of which are about how to be at home with the partner.

4.4 Experiment using metropolis traffic census data set

We also applied proposed DeepTMR to metropolis traffic census data set from e-Stat [1]. The rows and columns of the relational data matrix of this data set represent the locations of the metropolitan area in Japan, and each (i, j) th entry shows the number of people commuting (to work or school) one way from the i th location to the j th location per day. We removed the rows and columns that represent unknown locations (e.g., “unknown below Tokyo”) and total of multiple locations (e.g., “total of three wards in central Tokyo”) from the original data set. Let $A^{(0)} \in \mathbb{R}^{n \times p}$ be the matrix after removing such rows and columns, where $n = p = 249$. To alleviate the significant difference between the entry values and take relatively small entry values into account, we defined a matrix $A^{(1)} \in \mathbb{R}^{n \times p}$ whose entry is given by $A_{ij}^{(1)} = \log(A_{ij}^{(0)} + 1)$ for $i = 1, \dots, n$, and $j = 1, \dots, p$.

As in Sections 4.1 and 4.3, we define observed matrix A by replacing $\bar{A}^{(0)}$ and \bar{A} with $A^{(1)}$ and A , respectively. Then, we applied proposed DeepTMR to the observed matrix A , and checked the latent row-column structure of matrix A that was extracted by the DeepTMR. The hyperparameter settings for training proposed DeepTMR are given in Table 1.

Figures 15 and 16, respectively, show the results of matrices A , \underline{A} , \hat{A} , and vectors \mathbf{g} , \mathbf{h} , $\underline{\mathbf{g}}$, $\underline{\mathbf{h}}$ for this data set. Correspondence of row and column indices with locations in Figure 15 is given in Appendix B. The reordered input and output matrices \underline{A} and \hat{A} , respectively, show that the number of commuting people increases from the lower right to the upper left of the matrices. For instance, regardless of the home location, the number of people commuting to the locations in (C21) to (C25) (e.g., Nogi Town in Tochigi Prefecture, Tomisato City in Chiba Prefecture, and Fukaya City in Saitama Prefecture) in matrices \underline{A} and \hat{A} is relatively small. On the other hand, relatively many people commutes to the locations in (C1) (e.g., Minato-ku, Chiyoda-ku, and Shinjuku-ku in Tokyo), especially from the home locations in (R1) to (R10) (e.g., Setagaya-ku, Nerima-ku, and Machida City in Tokyo).

5 Discussion

Here we discuss the obtained results and the future directions of this study. In the experiments in Section 4, we showed that proposed DeepTMR could successfully reorder both synthetic and practical data matrices and provide their denoised mean matrices as output. Despite its effectiveness, proposed DeepTMR has a room for further improvement, as we describe in the subsequent paragraphs.

One potential merit of proposed DeepTMR to the other spectral and dimension-reduction-based methods is that it only requires the n -dimensional column data vector and p -dimensional row data vector as input, not the entire data matrix. This fact suggests the possibility that, in case that a set of rows or columns in a data matrix increases with time, we would not have to train proposed DeepTMR from scratch. Instead, we could only fine-tune the previously trained model with a newly added data for predicting their orders. A main problem in realizing this is that the input dimensions of the current DeepTMR should be fixed in advance. To apply the DeepTMR to such a time-series data matrix, we need to extend the DeepTMR so that it can accept a variable-length input data vector. Such an extension is also desirable in the perspective of memory cost. For a large data matrix, the DeepTMR model with an $(n + p)$ -dimensional input layer requires a huge amount of memory to be stored. One possible solution for this problem is to first randomly select k rows and h columns, where $k \ll n$ and $h \ll p$, and use the selected rows and columns as an input to the model. In this case, we need to develop a model in a different problem setting from ours, where each entry in an input data vector does not necessarily correspond to the same row or column.

Another limitation of the proposed method is that the trained DeepTMR model is affected by the random initialization, the mini-batch selection in each iteration, and the hyperparameter settings (e.g., number of units in each layer). In the experiment in Section 4.2, to partially alleviate this problem,

we trained the neural network multiple times and chose the result with the minimum training error. However, such a naive approach increases the overall computation time. It would be desirable if we can construct more sophisticated model, which is more robust to the effect of these settings. Particularly, it is an important future work to seek an optimal architecture of a neural network for a given data matrix. From the experimental results in Section 4, it has been shown that proposed DeepTMR could successfully extract the denoised mean matrices of input matrices with the sizes ranging from 100×100 to 249×249 by using the row/column encoder networks with 10 units in the middle layer. Based on these results, we expect that we do not always need to set the size of the DeepTMR network as large as the input matrix size to extract the structural patterns in a data matrix.

Finally, it would be interesting if we can utilize additional input information of rows and columns, aside from the entry values of an observed matrix. For instance, in the case of metropolis traffic census data set [1], which we used in Section 4.4, each row or column corresponds to a specific location in Japan. If we could extend proposed DeepTMR to reorder a data matrix using such additional row/column information (e.g., geographical location), it would be possible to obtain a different structural pattern about the data matrix from those provided by the current model.

6 Conclusion

In this paper, we proposed a new matrix reordering method DeepTMR based on a neural network model. By using an autoencoder-like architecture, proposed DeepTMR can automatically encode the row and column of an input matrix into one-dimensional nonlinear features, which can be later used for determining the row/column orders. Moreover, a trained DeepTMR model provides us with the denoised mean matrix as its output, which illustrates the global structure of the reordered input matrix. By experiments, we showed that proposed DeepTMR could successfully reorder the rows and columns of both synthetic and practical data sets, and that it could achieve higher accuracy in matrix reordering than the existing spectral and dimension-reduction-based matrix reordering methods based on SVD and MDS.

Acknowledgments

TS was partially supported by JSPS KAKENHI (18K19793, 18H03201, and 20H00576), Japan Digital Design, Fujitsu Laboratories Ltd., and JST CREST.

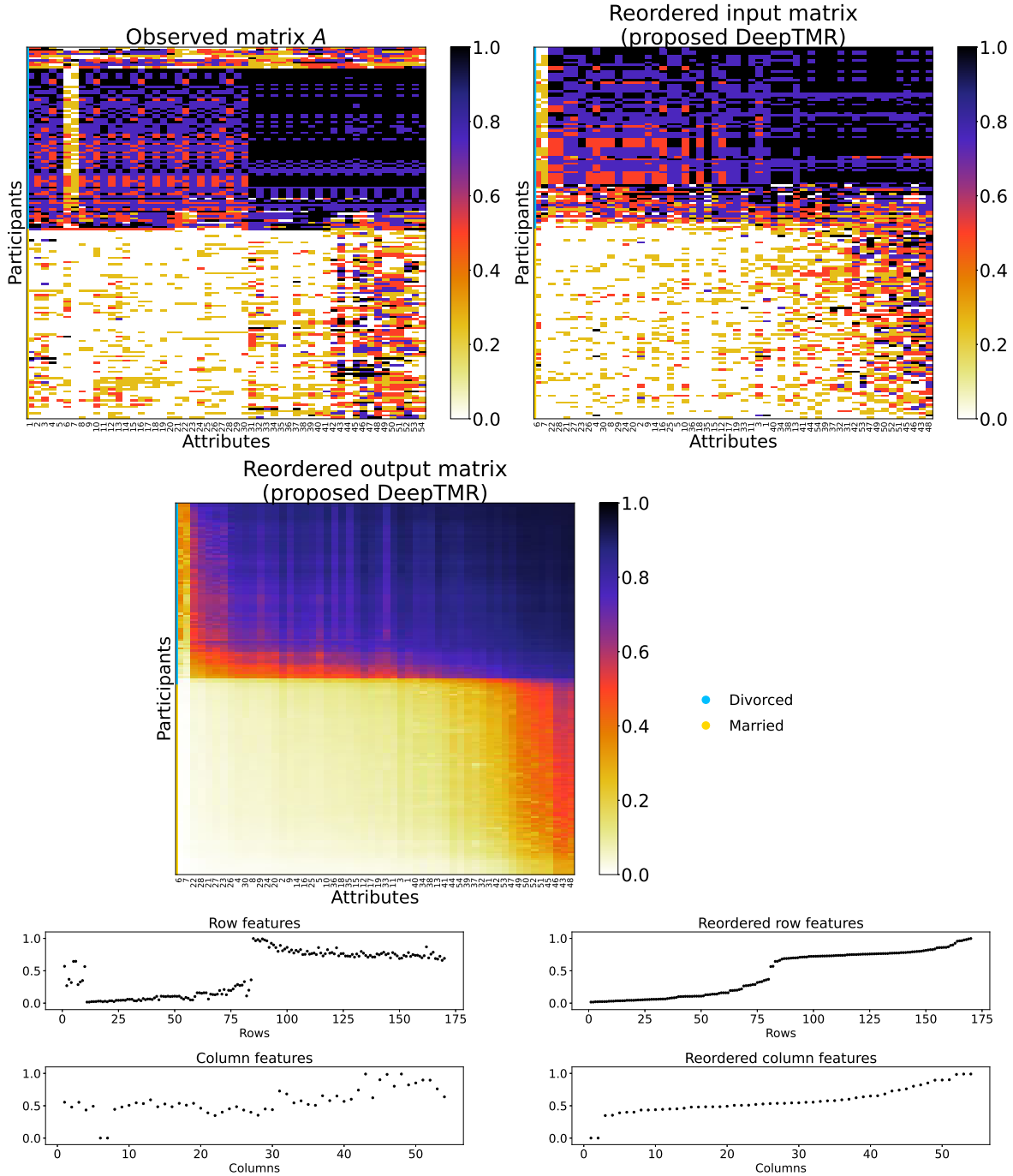


Figure 14: Results of the **Divorce Predictors data set**. Matrices A , \underline{A} , \hat{A} and vectors \mathbf{g} , \mathbf{h} , $\underline{\mathbf{g}}$, $\underline{\mathbf{h}}$.

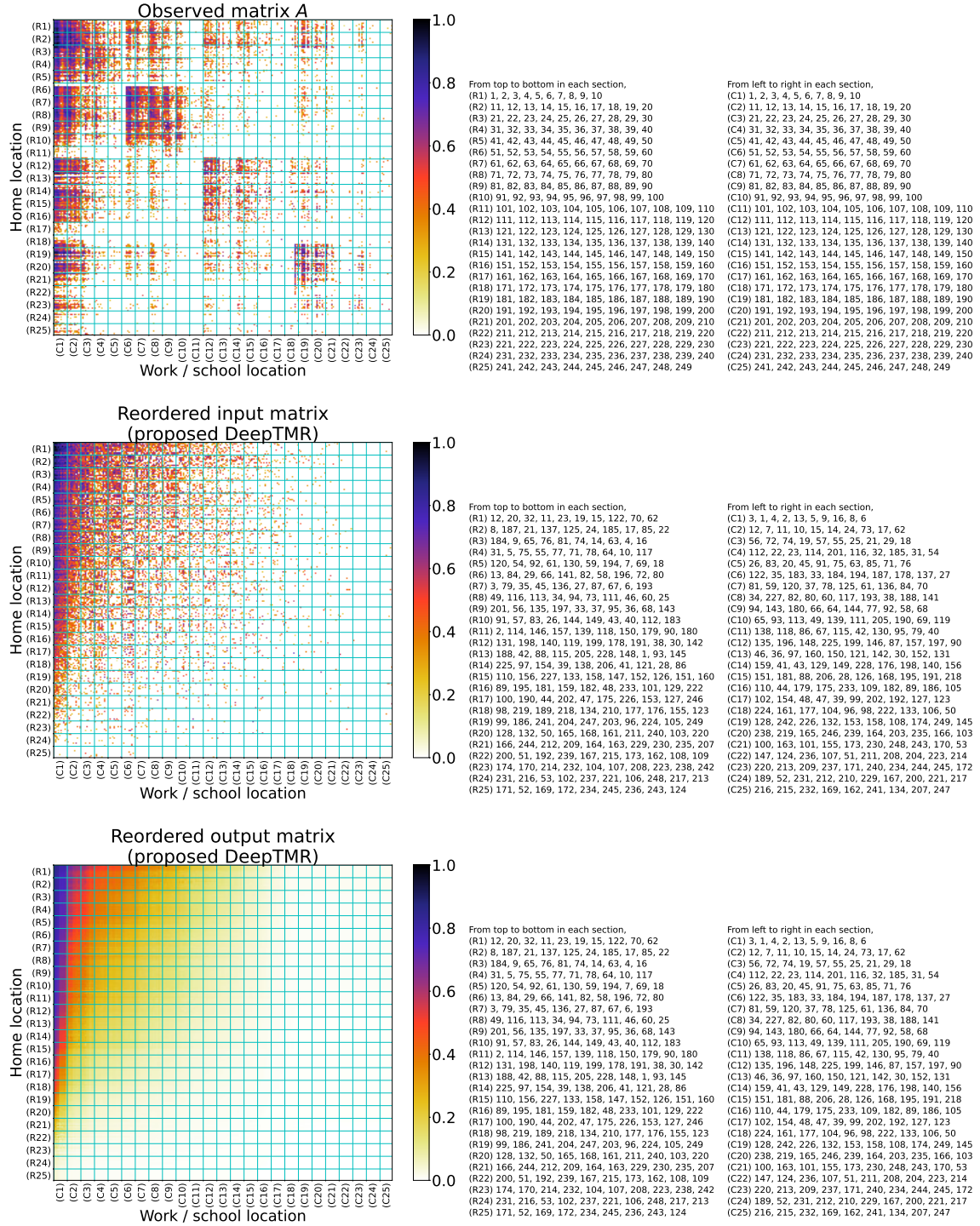


Figure 15: Results of the **metropolis traffic census data set**. Matrices A , and \hat{A} , \hat{A} . For visibility, we plotted cyan lines to show the sections between the sets of 10 rows or columns (i.e., $\{R1, \dots, R25\}$ and $\{C1, \dots, C25\}$ for rows and columns, respectively). Since the matrix size is $(n, p) = (249, 249)$, $R25$ and $C25$ contain 9 rows and 9 columns, respectively. Correspondence of indices with locations is given in Appendix B.

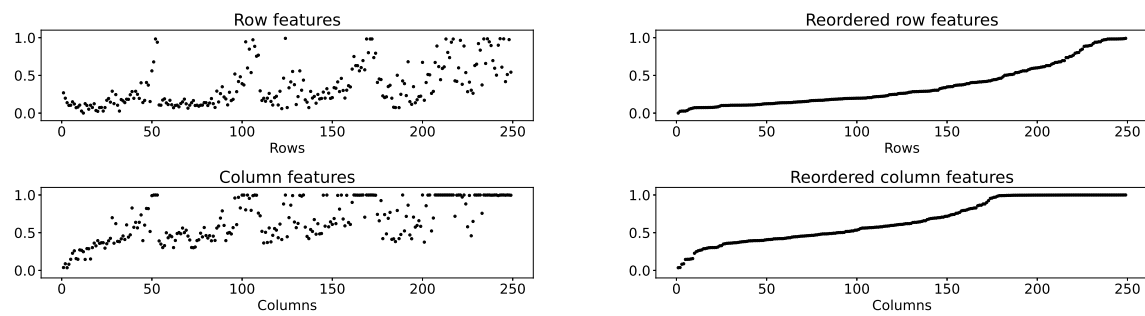


Figure 16: Results of the **metropolis traffic census data set**. Vectors g , h , \underline{g} , and \underline{h} .

Appendix A Correspondence of attribute indices with meanings in Divorce Predictors data set

The meaning of each attribute index of Divorce Predictors data set [31, 32] is as follows:

1. If one of us apologizes when our discussion deteriorates, the discussion ends.
2. I know we can ignore our differences, even if things get hard sometimes.
3. When we need it, we can take our discussions with my spouse from the beginning and correct it.
4. When I discuss with my spouse, to contact him will eventually work.
5. The time I spent with my wife is special for us.
6. We don't have time at home as partners.
7. We are like two strangers who share the same environment at home rather than family.
8. I enjoy our holidays with my wife.
9. I enjoy traveling with my wife.
10. Most of our goals are common to my spouse.
11. I think that one day in the future, when I look back, I see that my spouse and I have been in harmony with each other.
12. My spouse and I have similar values in terms of personal freedom.
13. My spouse and I have similar sense of entertainment.
14. Most of our goals for people (children, friends, etc.) are the same.
15. Our dreams with my spouse are similar and harmonious.
16. We're compatible with my spouse about what love should be.
17. We share the same views about being happy in our life with my spouse.
18. My spouse and I have similar ideas about how marriage should be.
19. My spouse and I have similar ideas about how roles should be in marriage.
20. My spouse and I have similar values in trust.
21. I know exactly what my wife likes.
22. I know how my spouse wants to be taken care of when she/he sick.
23. I know my spouse's favorite food.
24. I can tell you what kind of stress my spouse is facing in her/his life.
25. I have knowledge of my spouse's inner world.
26. I know my spouse's basic anxieties.
27. I know what my spouse's current sources of stress are.
28. I know my spouse's hopes and wishes.

29. I know my spouse very well.
30. I know my spouse's friends and their social relationships.
31. I feel aggressive when I argue with my spouse.
32. When discussing with my spouse, I usually use expressions such as 'you always' or 'you never.'
33. I can use negative statements about my spouse's personality during our discussions.
34. I can use offensive expressions during our discussions.
35. I can insult my spouse during our discussions.
36. I can be humiliating when we discussions.
37. My discussion with my spouse is not calm.
38. I hate my spouse's way of open a subject.
39. Our discussions often occur suddenly.
40. We're just starting a discussion before I know what's going on.
41. When I talk to my spouse about something, my calm suddenly breaks.
42. When I argue with my spouse, I only go out and I don't say a word.
43. I mostly stay silent to calm the environment a little bit.
44. Sometimes I think it's good for me to leave home for a while.
45. I'd rather stay silent than discuss with my spouse.
46. Even if I'm right in the discussion, I stay silent to hurt my spouse.
47. When I discuss with my spouse, I stay silent because I am afraid of not being able to control my anger.
48. I feel right in our discussions.
49. I have nothing to do with what I've been accused of.
50. I'm not actually the one who's guilty about what I'm accused of.
51. I'm not the one who's wrong about problems at home.
52. I wouldn't hesitate to tell my spouse about her/his inadequacy.
53. When I discuss, I remind my spouse of her/his inadequacy.
54. I'm not afraid to tell my spouse about her/his incompetence.

Appendix B Correspondence of indices with locations in metropolis traffic census data set

The meaning of each row or column index of metropolis traffic census data set [1] is as follows:

- **[Tokyo]** 1: Chiyoda-ku, 2: Chuo-ku, 3: Minato-ku, 4: Shinjuku-ku, 5: Bunkyo-ku, 6: Taito-ku, 7: Sumida-ku, 8: Koto-ku, 9: Shinagawa-ku, 10: Meguro-ku, 11: Ota-ku, 12: Setagaya-ku, 13: Shibuya-ku, 14: Nakano-ku, 15: Suginami-ku, 16: Toshima-ku, 17: Kita-ku, 18: Arakawa-ku, 19: Itabashi-ku, 20: Nerima-ku, 21: Adachi-ku, 22: Katsushika-ku, 23: Edogawa-ku, 24: Hachioji City, 25: Tachikawa City, 26: Musashino City, 27: Mitaka City, 28: Ome City, 29: Fuchu City, 30: Akishima City, 31: Chofu City, 32: Machida City, 33: Koganei City, 34: Kodaira City, 35: Hino City, 36: Higashimurayama City, 37: Kokubunji City, 38: Kunitachi City, 39: Fussa City, 40: Komae City, 41: Higashiyamato City, 42: Kiyose City, 43: Higashikurume City, 44: Musashimurayama City, 45: Tama City, 46: Inagi City, 47: Hamura City, 48: Akiruno City, 49: Nishitokyo City, 50: Mizuho Town, 51: Hinode Town, 52: Hinohara Village, 53: Okutama Town
- **[Yokohama City, Kanagawa Prefecture]** 54: Tsurumi-ku, 55: Kanagawa-ku, 56: Nishi-ku, 57: Naka-ku, 58: Minami-ku, 59: Hodogaya-ku, 60: Isogo-ku, 61: Kanazawa-ku, 62: Kohoku-ku, 63: Totsuka-ku, 64: Konan-ku, 65: Asahi-ku, 66: Midori-ku, 67: Seya-ku, 68: Sakae-ku, 69: Izumi-ku, 70: Aoba-ku, 71: Tsuzuki-ku
- **[Kawasaki City, Kanagawa Prefecture]** 72: Kawasaki-ku, 73: Saiwai-ku, 74: Nakahara-ku, 75: Takatsu-ku, 76: Tama-ku, 77: Miyamae-ku, 78: Asao-ku
- **[Sagamihara City, Kanagawa Prefecture]** 79: Midori-ku, 80: Chuo-ku, 81: Minami-ku
- **[Kanagawa Prefecture]** 82: Yokosuka City, 83: Hiratsuka City, 84: Kamakura City, 85: Fujisawa City, 86: Odawara City, 87: Chigasaki City, 88: Zushi City, 89: Miura City, 90: Hadano City, 91: Atsugi City, 92: Yamato City, 93: Isehara City, 94: Ebina City, 95: Zama City, 96: Minamiashigara City, 97: Ayase City, 98: Hayama Town, 99: Samukawa Town, 100: Oiso Town, 101: Ninomiya Town, 102: Nakai Town, 103: Oimachi, 104: Matsuda Town, 105: Kaisei Town, 106: Hakone Town, 107: Manazuru Town, 108: Yugawara Town, 109: Aikawa Town
- **[Saitama City, Saitama Prefecture]** 110: Nishi-ku, 111: Kita-ku, 112: Omiya-ku, 113: Minuma-ku, 114: Chuo-ku, 115: Sakura-ku, 116: Urawa-ku, 117: Minami-ku, 118: Midori-ku, 119: Iwatsuki-ku
- **[Saitama Prefecture]** 120: Kawagoe City, 121: Kumagaya City, 122: Kawaguchi City, 123: Gyoda City, 124: Chichibu City, 125: Tokorozawa City, 126: Hanno City, 127: Kazo City, 128: Honjo City, 129: Higashimatsuyama City, 130: Kasukabe City, 131: Sayama City, 132: Hanyu City, 133: Konosu City, 134: Fukaya City, 135: Ageo City, 136: Soka City, 137: Koshigaya City, 138: Warabi City, 139: Toda City, 140: Iruma City, 141: Asaka City, 142: Shiki City, 143: Wako City, 144: Niiza City, 145: Okegawa City, 146: Kuki City, 147: Kitamoto City, 148: Yashio City, 149: Fujimi City, 150: Misato City, 151: Hasuda City, 152: Sakado City, 153: Satte City, 154: Tsurugashima City, 155: Hidaka City, 156: Yoshikawa City, 157: Fujimino City, 158: Shiraoka City, 159: Ina Town, 160: Miyoshi Town, 161: Moroyama Town, 162: Ogose Town, 163: Namegawa Town, 164: Ranzan Town, 165: Ogawa Town, 166: Kawajima Town, 167: Yoshimi Town, 168: Hatoyama Town, 169: Tokigawa Town, 170: Yokoze Town, 171: Higashi Chichibu Village, 172: Misato Town, 173: Kamisato Town, 174: Yorii Town, 175: Miyashiro Town, 176: Sugito Town, 177: Matsubushi Town
- **[Chiba City, Chiba Prefecture]** 178: Chuo-ku, 179: Hanamigawa-ku, 180: Inage-ku, 181: Wakaba-ku, 182: Midori-ku, 183: Mihamaku

- **[Chiba Prefecture]** 184: Ichikawa City, 185: Funabashi City, 186: Kisarazu City, 187: Matsudo City, 188: Noda City, 189: Mobera City, 190: Narita City, 191: Sakura City, 192: Togane City, 193: Narashino City, 194: Kashiwa City, 195: Ichihara City, 196: Nagareyama City, 197: Yachiyo City, 198: Abiko City, 199: Kamagaya City, 200: Kimitsu City, 201: Urayasu City, 202: Yotsukaido City, 203: Sodegaura City, 204: Yachimata City, 205: Inzai City, 206: Shiroi City, 207: Tomisato City, 208: Katori City, 209: Sanmu City, 210: Oamishirasato City, 211: Shisui Town, 212: Sakae Town, 213: Kozaki Town, 214: Ichinomiya Town, 215: Chosei Village, 216: Nagara Town, 217: Otaki Town
- **[Ibaraki Prefecture]** 218: Tsuchiura City, 219: Koga City, 220: Ishioka City, 221: Yuki City, 222: Ryugasaki City, 223: Shimotsuma City, 224: Joso City, 225: Toride City, 226: Ushiku City, 227: Tsukuba City, 228: Moriya City, 229: Chikusei City, 230: Bando City, 231: Inashiki City, 232: Kasumigaura City, 233: Tsukubamirai City, 234: Miho Village, 235: Ami Town, 236: Kawachi Town, 237: Yachiyo Town, 238: Goka Town, 239: Sakai Town, 240: Tone Town
- **[Gunma Prefecture]** 241: Tatebayashi City, 242: Itakura Town, 243: Meiwa Town
- **[Tochigi Prefecture]** 244: Tochigi City, 245: Sano City, 246: Oyama City, 247: Nogi Town
- **[Yamanashi Prefecture]** 248: Otsuki City, 249: Uenohara City

References

- [1] e-Stat. https://www.e-stat.go.jp/stat-search/files?page=1&query=%E8%A1%8C%E6%94%BF%E5%8C%BA%E7%94%BB%E9%96%93%E7%BB%E5%8B%95%E4%BA%E5%93%A1%E8%A1%A8&layout=dataset&stat_infid=000031598030.
- [2] P. Arabie, S. A. Boorman, and P. R. Levitt. Constructing blockmodels: How and why. *Journal of Mathematical Psychology*, 17(1):21–63, 1978.
- [3] Z. Bar-Joseph, D. K. Gifford, and T. S. Jaakkola. Fast optimal leaf ordering for hierarchical clustering. *Bioinformatics*, 17(suppl_1):S22–S29, 2001.
- [4] M. Behrisch, B. Bach, N. H. Riche, T. Schreck, and J. Fekete. Matrix reordering methods for table and network visualization. *Computer Graphics Forum*, 35(3):693–716, 2016.
- [5] M. W. Berry, B. Hendrickson, and P. Raghavan. Sparse matrix reordering schemes for browsing hypertext. *Lectures in Applied Mathematics*, 32(2):99–123, 1996.
- [6] I. Borg and P. Groenen. *Modern Multidimensional Scaling: Theory and applications*. Springer Series in Statistics. Springer, New York, NY, 1997.
- [7] M. J. Brusco and S. Stahl. Using quadratic assignment methods to generate initial permutations for least-squares unidimensional scaling of symmetric proximity matrices. *Journal of Classification*, 17(2):197–223, 2000.
- [8] G. Caraux and S. Pinloche. PermutMatrix: a graphical environment to arrange gene expression profiles in optimal linear order. *Bioinformatics*, 21(7):1280–1281, 2005.
- [9] G. Cybenko. Approximation by superpositions of a sigmoidal function. *Mathematics of Control, Signals and Systems*, 2(4):303–314, 1989.
- [10] J. Díaz, J. Petit, and M. Serna. A survey of graph layout problems. *ACM Computing Surveys*, 34(3):313–356, 2002.
- [11] D. Dua and C. Graff. UCI machine learning repository. <http://archive.ics.uci.edu/ml>, 2017. University of California, Irvine, School of Information and Computer Sciences.
- [12] M. B. Eisen, P. T. Spellman, P. O. Brown, and D. Botstein. Cluster analysis and display of genome-wide expression patterns. *Proceedings of the National Academy of Sciences*, 95(25):14863–14868, 1998.
- [13] M. Friendly. Corrgrams: Exploratory displays for correlation matrices. *The American Statistician*, 56(4):316–324, 2002.
- [14] K.-I. Funahashi. On the approximate realization of continuous mappings by neural networks. *Neural Networks*, 2(3):183–192, 1989.
- [15] X. Glorot and Y. Bengio. Understanding the difficulty of training deep feedforward neural networks. In *Proceedings of the Thirteenth International Conference on Artificial Intelligence and Statistics*, volume 9 of *Proceedings of Machine Learning Research*, pages 249–256, 2010.
- [16] G. Govaert and M. Nadif. Clustering with block mixture models. *Pattern Recognition*, 36:463–473, 2003.
- [17] J. A. Hartigan. Direct clustering of a data matrix. *Journal of the American Statistical Association*, 67(337):123–129, 1972.

- [18] P. Ihm. A contribution to the history of seriation in archaeology. In *Classification — the Ubiquitous Challenge*, pages 307–316, 2005.
- [19] B. Irie and S. Miyake. Capabilities of three-layered perceptrons. In *IEEE 1988 International Conference on Neural Networks*, volume 1, pages 641–648, 1988.
- [20] D. P. Kingma and J. Ba. Adam: A method for stochastic optimization. In *3rd International Conference on Learning Representations*, 2015.
- [21] J. Y.-T. Leung, O. Vornberger, and J. D. Witthoff. On some variants of the bandwidth minimization problem. *SIAM Journal on Computing*, 13(3):650–667, 1984.
- [22] I. Liiv. Seriation and matrix reordering methods: An historical overview. *Statistical Analysis and Data Mining: The ASA Data Science Journal*, 3(2):70–91, 2010.
- [23] Y. Lin and J. Yuan. Profile minimization problem for matrices and graphs. *Acta Mathematicae Applicatae Sinica*, 10:107–112, 1994.
- [24] L. Liu, D. M. Hawkins, S. Ghosh, and S. S. Young. Robust singular value decomposition analysis of microarray data. *Proceedings of the National Academy of Sciences*, 100(23):13167–13172, 2003.
- [25] S. C. Madeira and A. L. Oliveira. Bioclustering algorithms for biological data analysis: a survey. *IEEE/ACM Transactions on Computational Biology and Bioinformatics*, 1(1):24–45, 2004.
- [26] W. M. F. Petrie. Sequences in prehistoric remains. *The Journal of the Anthropological Institute of Great Britain and Ireland*, 29(3/4):295–301, 1899.
- [27] W. S. Robinson. A method for chronologically ordering archaeological deposits. *American Antiquity*, 16(4):293–301, 1951.
- [28] J. L. Rodgers and T. D. Thompson. Seriation and multidimensional scaling: A data analysis approach to scaling asymmetric proximity matrices. *Applied Psychological Measurement*, 16(2):105–117, 1992.
- [29] I. Spence and J. Graef. The determination of the underlying dimensionality of an empirically obtained matrix of proximities. *Multivariate Behavioral Research*, 9(3):331–341, 1974.
- [30] A. Tanay, R. Sharan, and R. Shamir. Bioclustering algorithms: A survey. *Handbook of Computational Molecular Biology*, 9:1–20, 2005.
- [31] M. K. Yöntem. *The predictive role of the styles of parenthood origin on divorce predictors*. PhD thesis, Gaziosmanpasa University, 2017.
- [32] M. K. Yöntem, K. Adem, T. İlhan, and S. Kılıçarslan. Divorce prediction using correlation based feature selection and artificial neural networks. *Nevşehir HacıBektaş Veli Üniversitesi SBE Dergisi*, 9:259–273, 2019.
- [33] K. Zhao, Y. Rong, J. X. Yu, J. Huang, and H. Zhang. Graph ordering: Towards the optimal by learning. arXiv:2001.06631, 2020.